ELSEVIER

Journal of Molecular Catalysis A: Chemical 104 (1995) 171–177

JOURNAL OF MOLECULAR CATALYSIS A: CHEMICAL

Surface structure and acidity of alumina–boria catalysts

Satoshi Sato [a,*], Masakatsu Kuroki [b], Toshiaki Sodesawa [a], Fumio Nozaki [a], Gary E. Maciel [*,b]

[a] *Department of Applied Chemistry, Faculty of Engineering, Chiba University, Inage, Chiba 263, Japan*

[b] *Department of Chemistry, Colorado State University, Ft. Collins, CO 80523, USA*

Received 28 February 1995; accepted 16 May 1995

Abstract

Both surface borate structures and acidities of alumina–boria catalysts prepared by supporting B_2O_3 (boria) on an alumina support were investigated by using both ^{11}B magic angle spinning (MAS) NMR measurements and temperature-programmed desorption (TPD) of adsorbed pyridines, together with the catalytic properties of these alumina–boria materials for 1-butene isomerization. The concentrations of tetrahedral oxygen-coordinated borate (BO_4) species as well as number of Brønsted acid sites were found to increase with increasing boria content. The catalytic activity for 1-butene isomerization was found to be caused by the strong Brønsted acid sites generated from BO_4 species on the surface of alumina.

Keywords: ^{11}B MAS NMR; Alumina–boria; Acid sites; Brønsted acid sites

1. Introduction

An alumina–boria catalyst is one of the strong solid acid catalysts. It is readily prepared by impregnation methods using boric acid solution and an alumina support [1,2]. The acid behavior of alumina–boria is reported to be due to strong Brønsted acid sites [1,3]. The catalytic activities of alumina–boria are found to change with variation of the B_2O_3 (boria) content, and optimum boria contents have been found for such vapor-phase reactions as toluene disproportionation [1], *m*-xylene isomerization [3], and Beckmann rearrangement of cyclohexanone oxime [3,4].

Solid-state NMR techniques have been used to characterize structures of inorganic materials [5–9]. In the popular example of aluminosilicate zeolites [5], ^{27}Al and ^{29}Si NMR techniques provide useful information; coordination numbers of aluminum atoms are determined by ^{27}Al chemical shifts, and the microstructures of silicate centers, depending on the neighboring environment, are examined by ^{29}Si signals. In particular, these techniques are effective in studying surface structures of amorphous solids, such as silica gels [6,7], silica–alumina [8], and alumina [9]. Although ^{11}B NMR has been used frequently for organoborane and haloborate compounds in the liquid state [10,11], solid state ^{11}B NMR applications were used only for the characterization of such materials as glasses, ceramics and zeolites. In Pyrex glasses [12–14] and zeolites [15,16], ^{11}B NMR was used to detect tetrahedral oxygen-coordinated borate (BO_4) units in the complex patterns due to the quadrupole interaction of planar BO_3 units. Recently, BO_4 signals have been sep-

* Corresponding author.

SSDI 1381-1169(95)00105-0

arated from those of BO_3 units by using a high-speed magic-angle spinning (MAS) technique, together with a high magnetic field [13,17].

We have developed an evaluation method for acid strength distribution of Brønsted acid sites by using temperature-programmed desorption (TPD) of adsorbed 2,6-dimethylpyridine (2,6-DMP) [18]. Since 2,6-DMP adsorbs only on Brønsted acid sites, an acid strength distribution of Brønsted acid sites was provided. The TPD technique can clarify the type, strength, and amount of acid sites for solid acids such as alumina and silica–alumina, by comparing a TPD profile of 2,6-DMP which adsorbs on Brønsted acid sites with that of 3,5-DMP which adsorbs on both Brønsted and Lewis acid sites. We have demonstrated that Lewis acid sites of alumina are changed into Brønsted acid sites, together with a change in the acid strength, with increasing silica deposited on the alumina [18].

Although the catalytic activities of alumina–boria were studied previously, neither the surface structure of boria deposited on alumina nor their acid strength distribution was clarified [1–4]. In this paper, we investigate both surface borate structures and acid strength distributions of alumina–boria catalysts with different boria content by using ^{11}B MAS NMR measurement and TPD of adsorbed pyridines, in connection with their catalytic properties for 1-butene isomerization.

2. Experimental

2.1. Samples

Each alumina–boria sample was prepared by a conventional impregnation method. An alumina sample, DC-2282 supplied by Dia Catalyst Ltd. (specific surface area; 203 m^2/g, pore volume; 0.80 ml/g), was immersed in an aqueous solution of boric acid (H_3BO_3), and then the solution was dried. The resulting sample was calcined at 300°C for 3 h.

Each silica–boria sample was prepared in the same manner as for alumina–boria. A silica gel supplied by J.T. Baker was used as a support; it had a specific surface area of 290 m^2/g.

Sodium borate ($Na_2B_4O_7 \cdot 10H_2O$) supplied by J.T. Baker was used as a reference.

2.2. NMR measurements

^{11}B MAS NMR spectra were recorded at 192.55 MHz on a Bruker AM-600 multinuclear spectrometer, while a MAS spinner was rotated at a rate of 10 kHz. The hand-made spinner had a volume of 0.096 cm^3. Repetition times of 0.2 s were allowed between 3.0 μs pulses, and 2000 free induction decays (FID) were accumulated per sample; the 90° pulse width for an aqueous sodium borate solution was 10.3 μs. ^{11}B chemical shifts (in ppm) reported in this article are referenced to BF_3 etherate.

2.3. TPD of adsorbed pyridines

A sample (20 mg) held with quartz wool in a quartz tube was evacuated at 500°C for 1 h prior to adsorption of pyridines. An excess amount of pyridine or 2,6-dimethylpyridine was injected at 200°C, followed by evacuation for 1 h. A TPD measurement was done from 200 to 700°C at a heating rate of 5 K/min in a nitrogen flow of 70 ml/min. The desorbed pyridines were detected by a conductivity cell immersed in aqueous sulfuric acid. A cumulative amount of desorbed pyridines as a function of the desorption temperature was detected, and then differentiated to give a TPD profile as an acid strength distribution [18].

2.4. Catalytic tests

The isomerization of 1-butene was carried out in a closed circulation system (reactor volume, 200 cm^3) under the conditions of a 1-butene initial pressure of 19 kPa at 0°C. Prior to the reaction, a catalyst sample (50 mg) was preheated at 500°C under reduced pressure (0.1 Pa). The catalytic activity was evaluated in terms of the first-order rate constant during the initial reaction period.

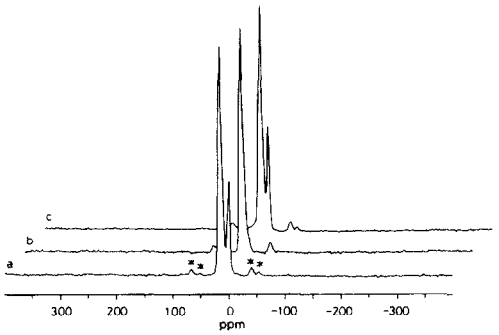

Fig. 1. ^{11}B MAS NMR spectra of alumina–boria catalysts treated under different conditions. The sample contained 7 wt.% of boria. a, without heat treatment; b, a calcined at 500°C for 3 h; c, b exposed to the ambient atmosphere for 24 h. * indicates a spinning side band.

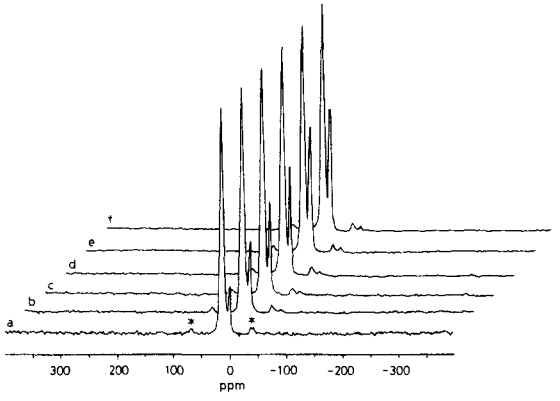

Fig. 2. ^{11}B MAS NMR spectra of alumina–borias with different boria contents. a, 3 wt.%; b, 5 wt.%; c, 7 wt.%; d, 10 wt.%; e, 15 wt.%; f, 20 wt.%. * indicates a spinning side band.

3. Results and discussion

3.1. ^{11}B NMR spectra of catalysts

Fig. 1 shows ^{11}B MAS NMR spectra of an alumina–boria sample with 7 wt.% of boria. It has 2 sharp resonance peaks at 1 and 15 ppm (Fig. 1-a), which are assigned as 4- and 3-coordinate boron sites (BO_4 and BO_3), respectively [13,17]. The sample was in the hydrated form because it had been stored open to the air after being calcined at 300°C. After the sample had been dehydrated by heating at 500°C for 3 h, the peak at 1 ppm disappeared (Fig. 1-b). The peak at 1 ppm recovered after exposure to the air for 24 h (Fig. 1-c). The NMR results show that the surface tetragonal BO_4 species are reversibly changed into trigonal BO_3 species during the hydration–dehydration process. Because of the instability of the BO_3 species in air, it is speculated that the surface BO_3 species that are produced by the dehydration of tetragonal BO_4 species are very strained.

Fig. 2 shows ^{11}B MAS NMR spectra of alumina–boria at different boria contents. Every sample had 2 sharp peaks at 1 and 15 ppm; the intensity of the peak at 1 ppm increased with an increase in boria content. Thus, the ratio of BO_4 to BO_3 species increases with increasing boria content. Turner et al. demonstrated that quantitatively reliable BO_4/BO_3 intensity ratios were obtained for several borate samples, using high-field ^{11}B MAS NMR [13]. In our preliminary experiments, BO_4/BO_3 intensity ratio in sodium borate ($Na_2B_4O_7 \cdot 10H_2O$) was found to be 1, which is the same as that reported by Turner et al. Therefore, we can determine the amounts of boria species quantitatively by using peak areas of ^{11}B NMR spectra. Accordingly, the concentrations of BO_3 and BO_4 species were calculated from the ratios of BO_3 to BO_4 species and the total boria content for each sample. The results are summarized in Table 1. Fig. 3 shows changes in the concentrations of BO_3 and BO_4 sites on the surface of the alumina–borias. Both the concentrations of BO_3 and BO_4 sites increased linearly with boria content. The line for BO_4 sites intersects the x-axis at 1.8 wt.% boria content. This fact will be

Table 1
Surface acidic properties of alumina–boria catalysts

Boria content	Concentration [a] of		2,6-DMP desorbed above		
wt.%	BO_3 mmol·g^{-1}	BO_4 mmol·g^{-1}	200°C [b] mmol·g^{-1}	400°C [c] mmol·g^{-1}	450°C [c] mmol·g^{-1}
0	–	–	0.007	0.002	0.001
3	0.74	0.12	0.028	0.003	0.002
5	1.18	0.26	0.043	0.004	0.001
7	1.56	0.45	0.072	0.015	0.005
10	2.16	0.72	0.085	0.022	0.011
15	3.12	1.19	0.116	0.025	0.008
20	4.16	1.58	0.116	0.015	0.003

[a] The values are the same as those in Fig. 2.
[b] The value is the same as that of Brønsted acid sites in Fig. 6.
[c] The values are the same as those in Fig. 8.

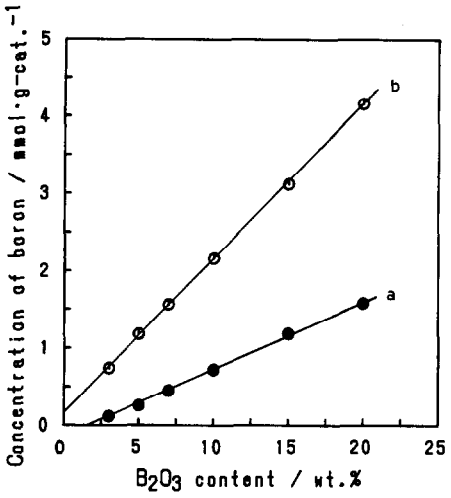

Fig. 3. Change in concentrations of boron sites with boria content. a, BO_4 species; b, BO_3 species.

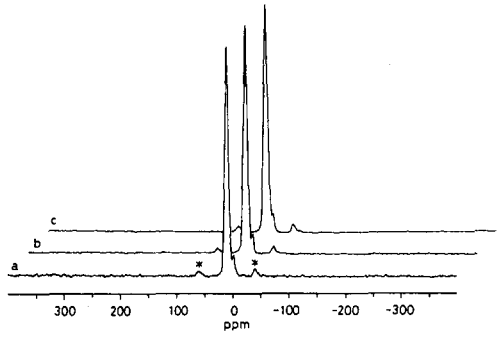

Fig. 4. ^{11}B MAS NMR spectra of silica–borias with different boria contents. a, 7 wt.%; b, 15 wt.%; c, 20 wt.%. * indicates a spinning side band.

discussed in connection with results of TPD (Fig. 8).

Fig. 4 shows ^{11}B MAS NMR spectra of hydrated silica–borias. These silica–boria samples also display both BO_4 and BO_3 sites at 1 and 15 ppm, respectively. In the same manner as for the alumina–boria case shown in Fig. 1, the BO_4 species at 1 ppm disappeared under heat treatment at 500°C, and the BO_4 species were recovered after adsorption of water (spectra not shown). In contrast to the NMR spectra of alumina–boria shown in Fig. 2, the intensity of BO_4 species at 1 ppm was weak and the ratio of intensities of BO_4 to BO_3 was constant regardless of boria content. Thus, the silica–boria samples are dominated by BO_3 sites. Boria is known to be one of the most difficult substances to crystallize, and in the vitreous state the structure consists of a 3-D network of partially ordered trigonal BO_3 units [19,20]. The NMR results of silica–boria indicate that the surface boria species are free boria, which has weak interactions with silica support.

3.2. TPD of adsorbed pyridines

Fig. 5 shows comparisons of TPD spectra of pyridine and 2,6-dimethylpyridine (2,6-DMP) adsorbed on alumina–boria at different boria contents. For alumina used as a support there are two broad desorption peaks of pyridine at around 320 and 660°C (Fig. 5-a), whereas small desorption peaks of 2,6-DMP were observed around 260 and 500°C (Fig. 5-b). The peaks of 2,6-DMP are caused by desorption from weak Brønsted acid sites [18]. Pyridine was also used instead of 3,5-

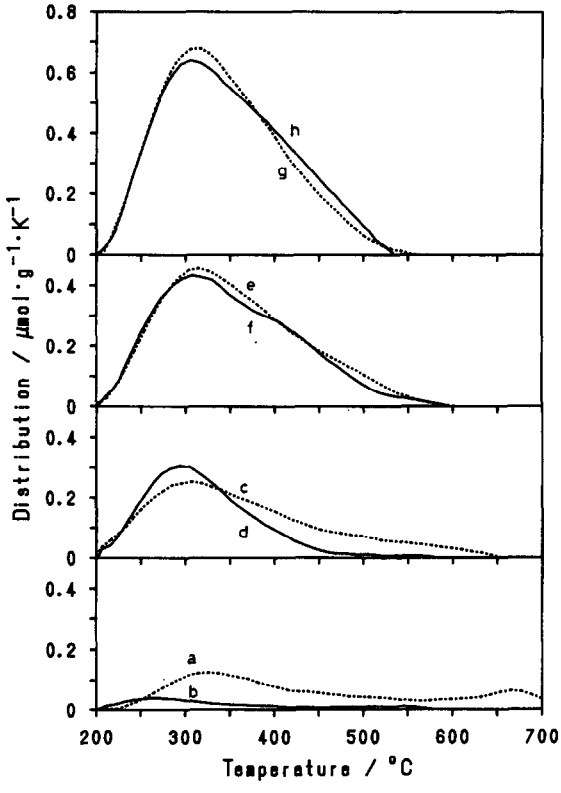

Fig. 5. Comparison of TPD profiles of 2,6-dimethylpyridine and pyridine adsorbed on alumina–boria with different boria contents. Dotted curves show TPD profiles of pyridine (a, c, e, and g), and solid curves are for 2,6-dimethylpyridine (b, d, f, and h). a and b, alumina; c and d, alumina–boria with 5 wt.% boria; e and f, 10 wt.%; g and h, 15 wt.%.

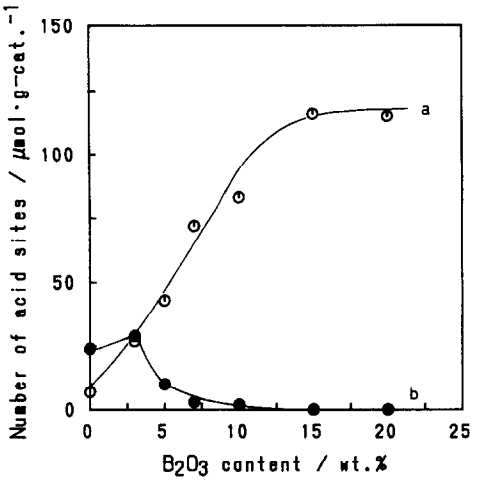

Fig. 6. Dependence of the number of acid sites of alumina–boria on the boria content. a, Brønsted acid sites; b, Lewis acid sites.

dimethylpyridine in this work, because it can adsorb on both Brønsted and Lewis acid sites. The significant difference between TPD curves of pyridine and 2,6-DMP indicates that Lewis acid sites dominate the alumina surface. The amount of 2,6-DMP desorbed from a sample containing 5 wt.% of boria (Fig. 5-d) was larger than that of alumina (Fig. 5-b). This indicates that Brønsted acid sites are created on the alumina surface by depositing boria species. Since the difference between the TPD curves of pyridine and 2,6-DMP (Fig. 5-c and d) is contributed by Lewis acid sites, the sample with 5 wt.% boria has both Lewis and Brønsted acid sites. At the higher boria contents of 10 and 15 wt.%, there was no significant difference between the two TPD curves of pyridine and 2,6-DMP (Fig. 5-e, f and 5-g, h). Thus, the alumina–boria samples have only Brønsted acid sites. Since the amount of pyridine desorbed increases with boria content (Fig. 5-a, c, e, g), the total number of acid sites increases with an increase in boria content.

Fig. 6 shows changes in the amounts of both Brønsted and Lewis acid sites with boria loading. The amount of Lewis acid sites, which was calculated from the difference between the amount of desorbed pyridine and desorbed 2,6-DMP, showed a maximum at a boria content of 3 wt.%; above this content it decreased slightly with increasing boria loading. On the other hand, the amount of Brønsted acid sites calculated from the desorption of 2,6-DMP increased linearly with increasing boria content. Izumi and Shiba measured the acidity of alumina–boria in terms of both the total acidity, determined by titration with n-butylamine, and Lewis acidity, measured by the chemisorption of triphenylmethyl chloride [1]. Their results are consistent with our results shown in Fig. 6. In contrast to alumina–boria, silica–boria showed a small amount (0.003 mmol·g^{-1}) of adsorbed 2,6-DMP at 7 wt.% of boria. Because pyridine adsorbs on silica–boria samples [21], Lewis acid sites were dominant on the silica–boria samples. The number of Brønsted acid sites of alumina–boria (Fig. 6), as well as the concentration of BO_4 species (Fig. 3), increase with increasing boria content. This indicates that the Brønsted acid sites of alumina–boria catalysts are correlated to the BO_4 species. The ratio of the total number of Brønsted acid sites to the number of BO_4 sites, however, changed from about two fifths to one tenth, comparing the third and fourth columns of Table 1.

Fig. 7 shows the variation in the Brønsted acid-strength distribution measured by the desorption of 2,6-DMP. At a small boria content of 3 wt.% (Fig. 7-b), the amount of 2,6-DMP desorbed near 300°C was drastically increased by depositing this small amount of boria on the surface of alumina (Fig. 7-a). A further increase in boria content induced an increase in the number of strong Brønsted acid sites, represented by desorption of

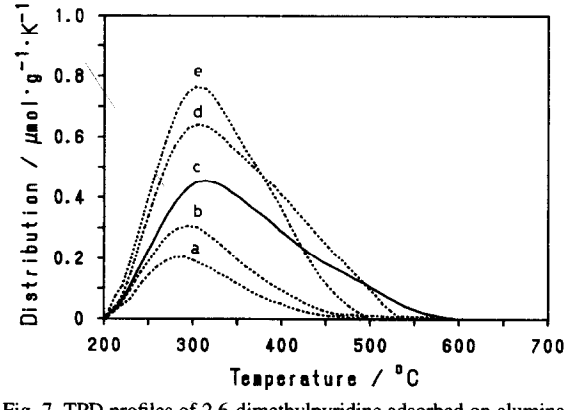

Fig. 7. TPD profiles of 2,6-dimethylpyridine adsorbed on alumina–boria. a, boria 3 wt.%; b, 5 wt.%; c, 10 wt.%; d, 15 wt.%; e, 20 wt.%.

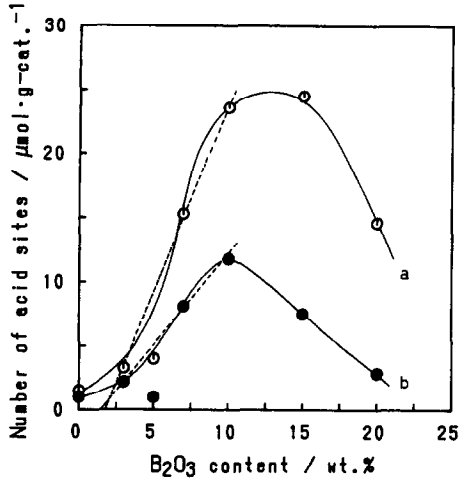

Fig. 8. Variation in the number of strong Brønsted acid sites with boria content. a, amount of 2,6-dimethylpyridine desorbed above 400°C; b, above 450°C.

2,6-DMP at temperatures higher than 400°C (solid curve of Fig. 7-c); the highest acid strength was attained at a boria content of 10 wt.%. Although the total amount of 2,6-DMP desorbed from a sample containing 15 wt.% boria was larger than that of the 10 wt.% boria sample, the acid strength was decreased because the sample had no distribution above 530°C (Fig. 7-d). A further decrease in acid strength was observed at a boria content of 20 wt.% because of no distribution above 500°C (Fig. 7-e).

Table 1 summarizes the surface acidic properties of alumina–boria catalysts together with the concentrations of BO_3 and BO_4 sites. The numbers of strong Brønsted acid sites from which 2,6-DMP desorbed at temperatures higher than 400 and 450°C were calculated by using the TPD curves shown in Fig. 7. Fig. 8 demonstrates the variation in the numbers of strong Brønsted acid sites. The variation show maxima at boria contents of about 10 wt.%. In this figure, two broken lines through the three points for 3, 7, and 10 wt.% boria samples cross the x-axis at about 2 wt.% boria. As shown in Fig. 3, the line for BO_4 species also crosses the x-axis at 1.8 wt.% boria content. This correspondence indicates that, at boria contents less than 10 wt.%, strong Brønsted acid sites of alumina–boria catalysts are correlated to surface BO_4 sites.

3.3. Catalytic activities for 1-butene isomerization

Catalytic activity for the isomerization of 1-butene is shown in Fig. 9. The catalytic activity changes with boria content, and is maximized at a boria content of 10 wt.%, which corresponds to a boria density of 0.5 $mg \cdot m^{-2}$. The alumina–boria system exhibits different catalytic activities for several reactions; maximum activities arise at surface boria densities of 0.6, 0.7, and 1.2 $mg \cdot m^{-2}$ for vapor-phase toluene disproportionation [1], *m*-xylene isomerization [3], and Beckmann rearrangement of cyclohexanone oxime [3,4], respectively. The value of 0.5 $mg \cdot m^{-2}$ for 1-butene isomerization is similar to those for the toluene disproportionation and *m*-xylene isomerization. These small values are typical for reaction catalyzed by strong Brønsted acid sites.

A good correlation between catalytic activity for 1-butene isomerization and Brønsted acidity measured by 2,6-DMP desorption has been reported for silica–alumina catalysts [18]. This reaction is catalyzed by strong Brønsted acid sites from which 2,6-DMP desorbs at temperatures higher than 400°C. On the other hand, silica–boria samples have no catalytic activity for this reaction, because they have no strong Brønsted acid sites from which 2,6-DMP could desorb above 400°C. The variation in catalytic activity of the alumina–

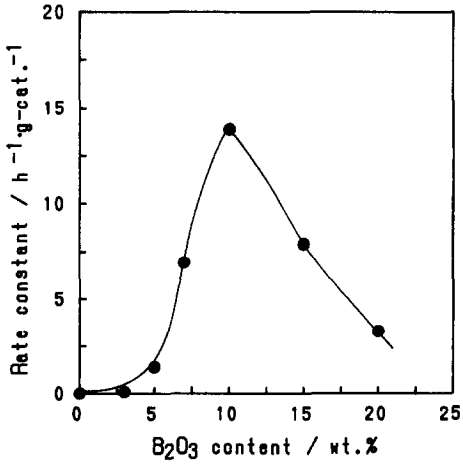

Fig. 9. Dependence of the catalytic activities for 1-butene isomerization at 0°C on the boria content of alumina–borias.

boria system, as represented in Fig. 9, is very similar to curve b in Fig. 8. This shows that much stronger Brønsted acid sites, on which pyridine can adsorb even at a temperatures of 450°C, are efficient for 1-butene isomerization.

In conclusion, the catalytic activity of alumina–boria is explained by the strong Brønsted acid sites generated from BO_4 species on the surface of alumina.

Acknowledgements

We thank Dr. S.F. Dec, Colorado State University, for assisting in the NMR measurements. One of the authors (Sato) expresses his thanks to the Ministry of Education of Japan for the financial support of his NMR study at Colorado State University as an overseas researcher.

References

[1] Y. Izumi and T. Shiba, Bull. Chem. Soc. Jpn., (1964) 1797.
[2] Y. Murakami, Y. Saeki and K. Ito, Nippon Kagaku Kaishi, (1978) 21.
[3] H. Sakurai, S. Sato, K. Urabe and Y. Izumi, Chem. Lett., (1985) 1783.
[4] S. Sato, S. Hasebe, H. Sakurai, K. Urabe and Y. Izumi, Appl. Catal., 29 (1987) 107.
[5] G. Engelhardt and D. Michel, High-Resolution Solid-State NMR of Silicates and Zeolites, John Wiley & Sons, 1987, p. 332.
[6] G.E. Maciel and D.W. Sindorf, J. Am. Chem. Soc., 102 (1980) 7606.
[7] I.-S. Chuang, D.R. Kinney, C.E. Bronnimann, R.C. Zeigler and G.E. Maciel, J. Phys. Chem., 96 (1992) 4027.
[8] S. Sato, T. Sodesawa, F. Nozaki and H. Shoji, J. Mol. Catal., 66 (1991) 343.
[9] D. Coster, A.L. Blumenfeld and J.J. Fripiat, J. Phys. Chem., 98 (1994) 6201.
[10] R.G. Kidd, NMR of Newly Accessible Nuclei, Vol. 2, Academic Press, New York, 1983, p. 49.
[11] A.R. Siedle, Annu. Rep. NMR Spectrosc., 20 (1988) 205.
[12] C.A. Fyfe, G.C. Gobbi, J.S. Hartman, R.E. Lenkinski, J.H. O'Brien, E.R. Beange and M.A.R. Smith, J. Magn. Reson., 47 (1982) 168.
[13] G.L. Turner, K.A. Smith, R.J. Kirkpatrick and E. Oldfield, J. Magn. Reson., 67 (1986) 544.
[14] J. Zhong and P.J. Bray, J. Non-Cryst. Solids, 111 (1989) 67.
[15] L.A. Vostrikova, K.G. Ione, V.M. Mastikhin and A.V. Petrova, React. Kinet. Catal. Lett., 26 (1984) 291.
[16] K.F.M.G.J. Scholle and W.S. Veeman, Zeolites, 5 (1985) 118.
[17] S.F. Dec and G.E. Maciel, J. Magn. Reson., 87 (1990) 153.
[18] S. Sato, M. Tokumitsu, T. Sodesawa and F. Nozaki, Bull. Chem. Soc. Jpn., 64 (1991) 1005.
[19] Comprehensive Inorganic Chemistry, Vol. 1, 1st Ed., Pergamon Press, New York, 1973, p. 880.
[20] A.F. Wells, Structural Inorganic Chemistry, 5th Ed., Clarendon Press, Oxford, 1984 p. 1065.
[21] S. Sato, K. Urabe and Y. Izumi, J. Catal., 102 (1986) 99.